Kim, Maria; Shah, Ali; Li, Changfeng; Mustonen, Petri; Susoma, Jannatul; Manoocheri, Farshid; Riikonen, Juha; Lipsanen, Harri

Direct transfer of Wafer-scale graphene films

Published in:
2 D Materials

DOI:
10.1088/2053-1583/aa780d

Published: 01/09/2017

Document Version
Publisher's PDF, also known as Version of record

PAPER • **OPEN ACCESS**

Direct transfer of wafer-scale graphene films

To cite this article: Maria Kim *et al* 2017 *2D Mater.* **4** 035004

2D Materials

OPEN ACCESS

RECEIVED
1 June 2017

ACCEPTED FOR PUBLICATION
8 June 2017

PUBLISHED
22 June 2017

PAPER

Direct transfer of wafer-scale graphene films

Maria Kim[1], **Ali Shah**[1], **Changfeng Li**[1], **Petri Mustonen**[1], **Jannatul Susoma**[1], **Farshid Manoocheri**[2], **Juha Riikonen**[1] **and Harri Lipsanen**[1]

[1] Department of Electronics and Nanoengineering, Aalto University, PO Box 13500, FI-00076 Aalto, Finland
[2] Metrology Research Institute, Aalto University, PO Box 15500, FI-00076 Aalto, Finland

E-mail: maria.grigoryeva@aalto.fi

Keywords: graphene, flexible electronics, electrical conductivity, transparency, two-dimensional material, parylene-C

Supplementary material for this article is available online

Abstract

Flexible electronics serve as the ubiquitous platform for the next-generation life science, environmental monitoring, display, and energy conversion applications. Outstanding multi-functional mechanical, thermal, electrical, and chemical properties of graphene combined with transparency and flexibility solidifies it as ideal for these applications. Although chemical vapor deposition (CVD) enables cost-effective fabrication of high-quality large-area graphene films, one critical bottleneck is an efficient and reproducible transfer of graphene to flexible substrates. We explore and describe a direct transfer method of 6-inch monolayer CVD graphene onto transparent and flexible substrate based on direct vapor phase deposition of conformal parylene on as-grown graphene/copper (Cu) film. The method is straightforward, scalable, cost-effective and reproducible. The transferred film showed high uniformity, lack of mechanical defects and sheet resistance for doped graphene as low as 18 Ω/sq and 96.5% transparency at 550 nm while withstanding high strain. To underline that the introduced technique is capable of delivering graphene films for next-generation flexible applications we demonstrate a wearable capacitive controller, a heater, and a self-powered triboelectric sensor.

1. Introduction

The discovery of graphene was a breakthrough in the material science [1]. The excellent electrical, physical and chemical properties [2] gave rise to electronic applications, such as transparent electrodes [3], heaters [4], and graphene transistors [1, 5]. Owing to the atomically thin structure, high transmittance of ~97% at visible light [6] and flexibility are inherent advantages of graphene rendering it an excellent candidate for flexible and transparent applications. CVD graphene appears as a cost-effective method satisfying industrial requirements to utilize graphene in real-life applications since it enables the fabrication of uniform highly conductive monolayer films in wafer scale [7]. Compared to indium tin oxide (ITO), graphene offers high flexibility and tolerance against strain [3]. Thus, processing of graphene and harvesting its inherent properties is a precious research area. Development of CVD graphene transfer method on a flexible and transparent substrate discloses numerous areas for graphene application.

Typically, CVD graphene employs transition metals as substrates due to their enhanced catalytic behavior [2]. Cu foil is the most commonly used catalytic substrate for graphene growth as it is inexpensive and readily available compared to other transition metals. Additionally, Cu alleviates the synthesis of monolayer graphene as the growth process in limited to the surface by the low carbon solubility [2]. To capitalize the graphene properties, for most applications, the CVD film is transferred to an insulating substrate. The transfer is a critical part of the whole fabrication process as in part it determines the quality of the graphene film and the overall cost of the material.

The most frequently applied transfer method for CVD graphene relies on using polymethylmethacrylate (PMMA) as a temporary supporting membrane [8]. After the PMMA deposition on graphene, Cu can be removed by several techniques including chemical etching [2], peeling [9], or electrochemical delamination [10]. The process is finalized by placing the PMMA/graphene film onto a target substrate and dissolving PMMA in acetone. This laborious

polymer-based method suffers from drawbacks: it is non-scalable, requires several intermediate steps, minuscule PMMA residues are difficult to remove, skills of the individual performing the transfers affects the outcome, and PMMA is not suitable as a final substrate due to instability at high temperatures and inability to resist basic solvents. Recently, Zhang *et al* reported about usage of rosin ($C_{19}H_{29}COOH$) as a good support layer for graphene transfer, however, claiming only a decreased amount of residue from a polymer [11]. The elastomer stamps and self-releasing layers such as polydimethylsiloxane (PDMS) [9] and thermal release tape (TRT) [12], respectively, substitute PMMA carrier overcoming some drawbacks. However, these supporters require high adhesion between graphene and the destination surface. Otherwise, removal of the carrier can cause undesired mechanical defects in the graphene layer [13]. Thus, an increase of adhesion between the target substrate requires additional process steps without solving the issue of a temporary carrier substrate.

Roll-to-roll techniques have been introduced for large-scale graphene transfer using flexible substrates [3, 14]. Transfer includes three stages, applying hot rollers in each: adhesion of a supporting polymer film, Cu removal and transfer to a flexible substrate. Despite cost-efficiency and scalability, this method also employs carrier substrate and relies on high adhesion between graphene and the target substrates. Moreover, the roll-to-roll process can induce undesired stress to graphene leading to cracks and voids [3, 8]. As opposed to the transfer methods using intermediate carrier substrates, the target substrate can be directly attached to graphene on the Cu foil. This kind of direct transfer is straightforward as essentially the second, and the final step is the removal of Cu. However, the most famous and known substrates such as polyethylene terephthalate (PET), polystyrene (PS), epoxy, and other polymers are susceptible to heat degradation and their chemical and physical properties highly depend on processing condition. Further, removal of graphene from one side of Cu foil requires additional step as in these methods etchants remove Cu to minimalize stresses, but graphene grows on both sides of Cu in the CVD process. A fracture mechanics analysis and measurements of adhesion energy between graphene and Cu prove that graphene transfer requires careful selection of target substrate and highly conformal contact to avoid additional defects [13, 15].

In this work, we demonstrate a direct transfer of 6-inch monolayer CVD graphene based on CVD deposition of poly-para-xylylene polymer (known as parylene). The transferred films are highly transparent (96.5% at 550 nm), and the smallest achieved sheet resistance is 18 Ω/sq, whereas average sheet resistance over an area of $6 \times 6\,cm^2$ is 25 Ω/sq. The transferred film is robust showing invariable sheet resistance even upon 6% strain and bending to a radius of 250 μm. The transferred film is further employed to demonstrate a wearable capacitive controller, a heater, a touch panel, and a triboelectric sensor. The advantage of the method originates from the conformal deposition of parylene as it offers perfect support for CVD graphene despite intrinsic imperfections such as corrugations, wrinkles, and ripples. Considering that parylene is already widely utilized in the industry, we expect this transfer technique to results in whole new flexible and transparent graphene applications satisfying requirements of conformal coating and technical approach for graphene transfer.

2. Description of a graphene transfer method

Parylene has been employed for years in applications among military, aerospace, biomedicine and semiconductor industry. Military and US food and drug administration (FDA) have approved it for a huge number of applications such as a conformal coating for protecting equipment against environmental extremes, defibrillator membranes, and neural probes [16]. Parylene has several formulations including high-temperature and UV-stable variants. Deposition is extremely reproducible and safe as it performed at a room temperature and in a vacuum without solvents or hazardous substances. Consequently, it is widely adopted in the biomedical industry. Several research groups demonstrated various applications of parylene such as a substrate and/or coating for implantable biomedical devices [17, 18]. Recently, Park *et al* fabricated a graphene-based neural electrode, where parylene served as the substrate [19].

The semiconductor industry, on the other hand, employs parylene as an encapsulating, pinhole free layer against moisture with possibility to control thicknesses from nanometers to micrometers. Although, parylene was widely used as a gate dielectric in carbon nanotubes (CNT) based networks and composite films [20, 21]. To date, few reports demonstrate successful application of parylene in graphene encapsulation [22], gating of graphene-based field-effect transistor (FET) [23] and $MoSe_2$ FET [24]. Also, parylene was utilized as a substrate, however studies were limited to deposition of parylene on rigid or flexible substrates [25, 26]. Parylene was compared to the most common flexible substrates and underlined limitations for fabrication processes (see supporting information table S1) (stacks.iop.org/TDM/4/035004/mmedia). Thereby, the vast opportunities provided by the material itself and the vapor phase deposition at room temperature are explored for graphene transfer.

Figure 1(a) illustrates the direct transfer process demonstrated in this work. Monolayer CVD graphene utilized in the transfer process was grown on a 6-inch Cu foil (details in methods below). As the first step in the transfer process, Parylene-C was deposited directly on the as-grown graphene on Cu. It is to mention that, Parylene-C differs from natural parylene (Parylene-N) having one chlorine atom attached to the benzene

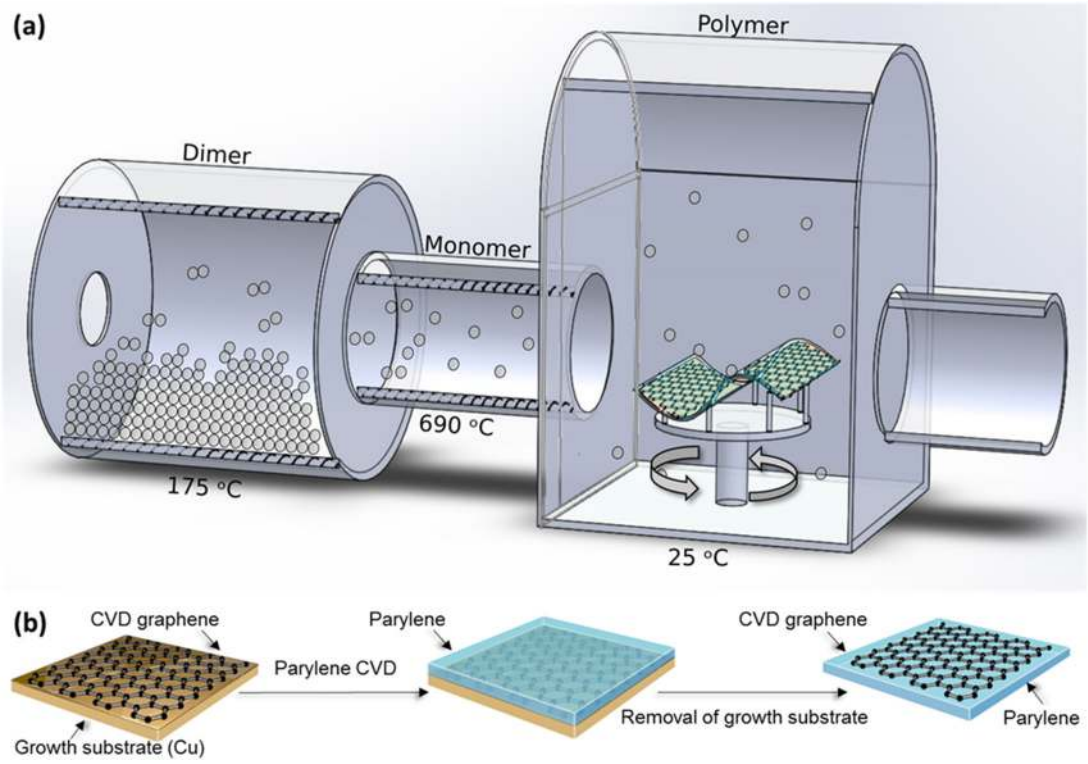

Figure 1. Parylene based transfer process: (a) schematic of the parylene deposition process. (b) Schematic of the parylene based graphene transfer.

ring. This chemical modification results in an advantageous combination of electrical and physical properties including particularly low moisture and gas permeability in addition to deposition rate faster than that of Parylene-N. During the deposition, parylene is initially vaporized from its solid dimer phase inside the vaporizer furnace at ~120 °C. Next, the pyrolysis occurs in a high-temperature furnace (>600 °C), which converts the dimers to monomers by breaking the methylene-methylene bonds. In the last stage, the polymerization of the monomer takes place at room temperature on the substrate surface inside the deposition chamber at the pressure of ~0.1 mbar. As the polymerization reaction is limited to the surface and the monomer can penetrate into convex portions of the surface and results in a parylene film that is highly conformal [27]. The direct deposition induces no physical or thermal stress to graphene from the gas phase at room temperature.

The second and the final step in the transfer process is Cu removal to achieve freestanding graphene/parylene film. To demonstrate the versatility of this transfer method, we removed Cu by three different methods: etching, electrochemical delamination and peeling (see supporting information figure S1).

Figure 1(b) shows the flow diagram of the applied graphene transfer technique. We mainly utilize the electrochemical delamination (bubbling transfer) as demonstrates an economic and environmental-friendly way of preparing high-quality CVD graphene via recycling the Cu substrate. Figure 2(a) shows a wafer scale transferred graphene on parylene.

2.1. Raman and SEM investigation

Confocal μ-Raman spectroscopy was used to characterize and confirm the quality of the transferred graphene. Figure 2(b) presents the Raman spectrum of the graphene/parylene film displaying clearly the 2D peak of graphene at ~2691 cm^{-1}. The FWHM of the 2D band (29.1 cm^{-1}) is consistent with of the Raman fingerprint of monolayer graphene [28]. Unfortunately, as parylene also contains benzene rings, Raman spectrum of parylene has peaks at ~1442 cm^{-1} and ~1609 cm^{-1}, which correspond to D and G peaks of graphene, respectively. This fact obviously limits the Raman analysis. SEM images in figure 2(c) show that the transferred graphene layers are highly continuous and uniform. To further test the method, we also transferred a non-continuous CVD graphene film, as the voids between the graphene grains are highly susceptible for rolling and cracking compared to a continuous film.

2.2. Enhancing of graphene conductivity

For further evaluation of the performance of transferred monolayer graphene, we employed graphene functionalization. Several different doping procedures and chemicals have been proposed and reported for graphene, CNTs, and other nanocarbon materials [29–32]. We utilized nitric acid (HNO_3) and gold chloride ($AuCl_3$) for doping as those are effective dopants for graphene [3, 32]. Some recent studies have also employed potassium and iodine as dopants by introducing them to the graphene surface via potassium adatoms [30], iodine ionic complexes [33], and iodine

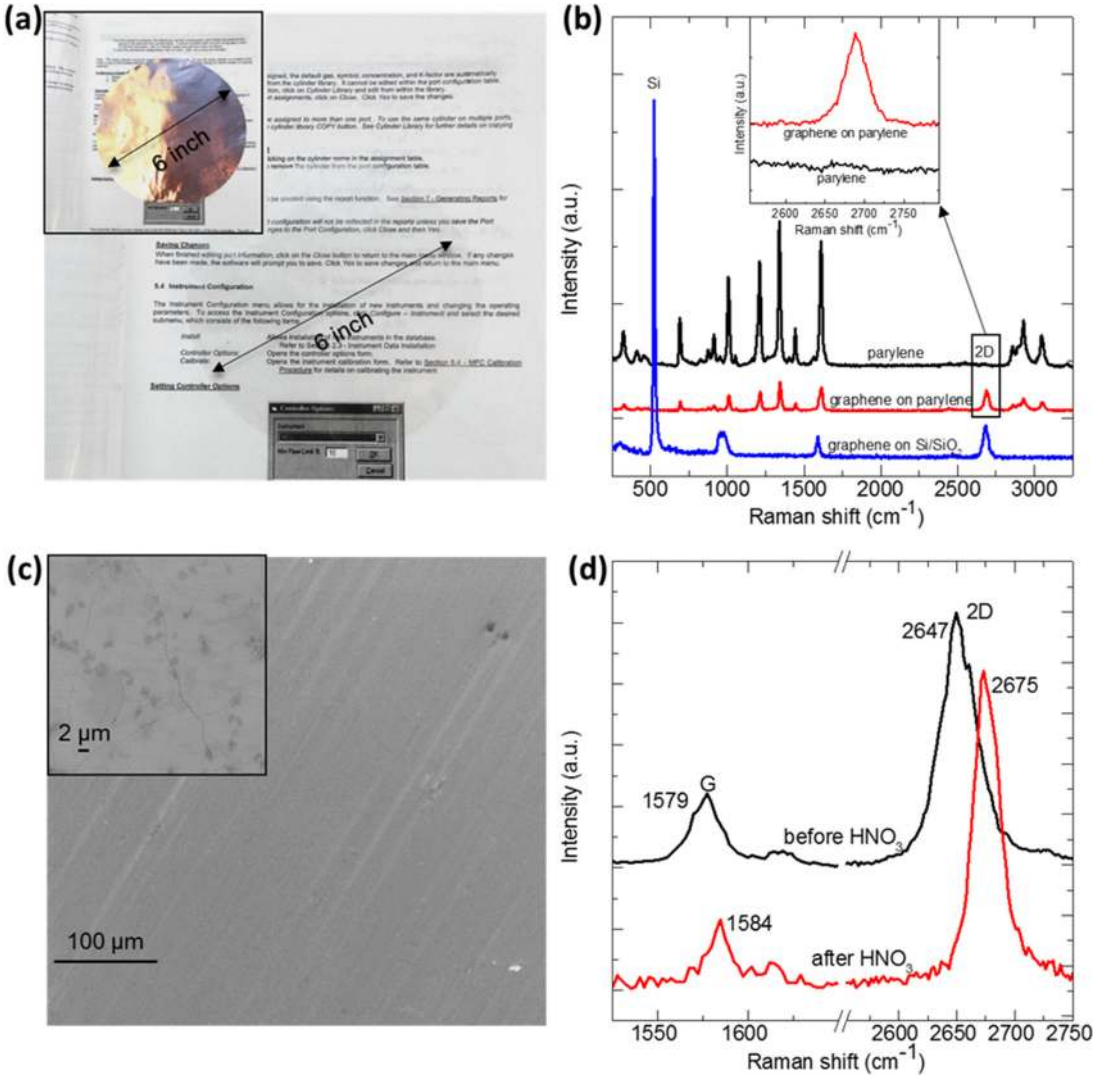

Figure 2. Optical characterization of graphene/parylene films: (a) graphene on 25 μm CVD deposited parylene after electrochemical delamination of Cu foil. (Inset) Graphene on Cu foil covered with 25 μm CVD deposited parylene. (b) Raman spectra of graphene/parylene film, parylene only and graphene on Si/SiO_2. The inset shows the spectrum around graphene 2D peak for parylene and graphene on parylene in detail. (c) SEM image of monolayer graphene on parylene with different magnifications. (d) Raman spectra of 2D and G band before and after HNO_3-doping.

mixture with camphor [31]. However, KI was not employed in those experiments, but there are studies where KI has been used to etch gold away from top of graphene [34]. There, the finding was that the graphene was not affected by KI. Due to this contradiction, we decided to study the effect of KI doping to the graphene/parylene films.

Sheet resistance was measured using four-probe system by pressing the probes directly to graphene without predeposited contacts. The distance between the probes is 1.5 mm, which is relatively large as it results in a measured area of several square millimeters. Consequently, the measurement provides a meaningful value for the sheet resistance as it takes into account several grain boundaries and possible defects in the graphene film. Therefore, it is expected to provide reliable value for the sheet resistance compared to patterned small scale devices.

Figure 2(d) shows Raman spectra of graphene films before and after 15 min doping with 69% HNO_3. The 2D peak shift of 28 cm^{-1} indicates strong p-type doping of graphene as expected [35]. The p-type doping with the chosen chemicals clearly enhances the conductivity of the graphene films. The lowest sheet resistance achieved by HNO_3 treatment is as low as 18 Ω/sq. The averaged value of the sheet resistance decreased from 150 Ω/sq to 25 Ω/sq by doping. Figure 3(a) shows the distribution of R_s measured from over 100 points of the 6 × 6 cm^2 graphene/parylene film before and after HNO_3 doping. The maps and histograms demonstrate increased spatial homogeneity in the sheet resistance due to chemical treatment. We attribute this enhancement to the removal of unintentional dopants (adatoms) and the ability of HNO_3 functionalization to provide uniform doping profile. Nitric acid provides covalent attachment of C–OH, C(O)OH and NO_3^- moieties to carbon atoms through sp^2–sp^3 hybridization resulting in the Fermi level shift towards p-type doping [36]. Graphene doped with KI and $AuCl_3$ also led to the enhancement of graphene conductivity; sheet

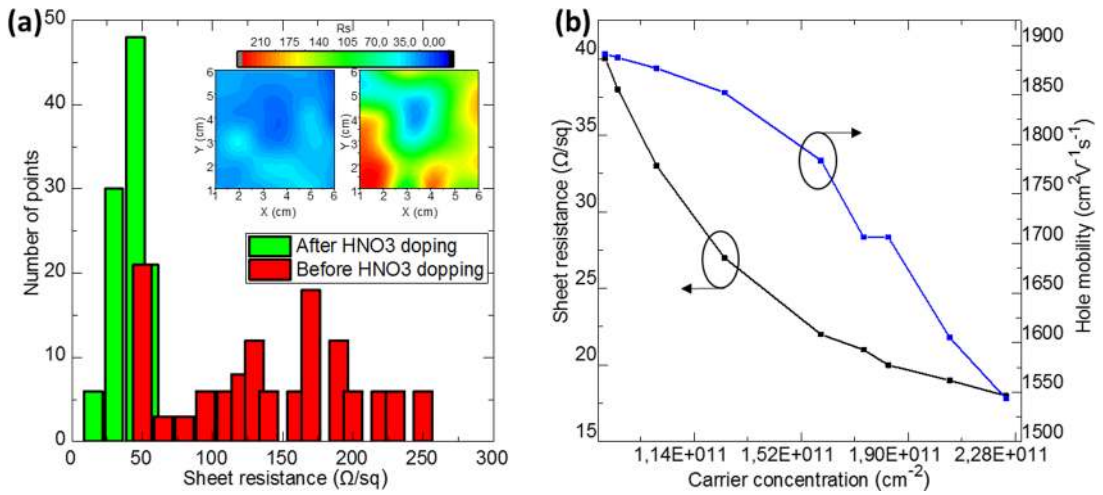

Figure 3. Electrical characterization of transferred and doped graphene: (a) dependence of sheet resistance on dopants. (b) Sheet resistance, charge carrier concentration and hole mobility values of the doped graphene.

resistance drops from 150 Ω/sq to 100 Ω/sq and 30 Ω/sq for KI and $AuCl_3$, respectively.

The sheet resistance values of the graphene/parylene films were confirmed by van der Pauw measurements 2 × 2 cm^2 control samples (as limited by the measurement setup). These samples were also used to perform Hall measurements, which showed hole mobility of ~1500 $cm^2\,V^{-1}\,s^{-1}$ at room temperature (figure 3(b)). High mobility for the large-area sample is also a clear evidence of high-quality graphene on parylene.

2.3. Transmission measurement

In addition to a low resistivity, high transmittance is paramount for transparent conductive layers. When analyzing transmittance of conducting films, it is important to note that these characteristics are in fact interconnected [37], as the response of electrons to either static (voltage) or dynamic (light) electric fields determines both R_s and T:

$$T = \left(1 + \frac{Z_0 Q_{op}}{2R_s Q_{DC}}\right)^{-2} \quad (1)$$

Where Z_0 is the impedance of free space, Q_{op} is optical conductivity, and Q_{DC} is DC conductivity. Thus conductivity ratio given by the equation controls dependence of T on R_s and, therefore, acknowledging the limits of desired properties. Q_{DC}/Q_{op} ratio can be considered as a figure-of-merit (FoM) for transparent conductors. Thus, the theoretical limitation of this ratio for graphene exceeds that for ITO and CNTs, which makes graphene very promising material in this research field [38].

Figure 4(a) presents empirical results achieved for transparent and conductive electrodes obtained in this work and previous studies [4, 9, 39–41]. Although, prior results display significant variation ranging from highly conductive to highly resistive films, here we have only included state-of-the-art films. Transmission values are substrate normalized, meaning that the value is the transmittance of the conductive film only. A graphene film transferred to PET by a soluble polymer support such as PMMA shows the highest transmittance of ~97.5% at 550 nm. However, the sheet resistance value after HNO_3 functionalization is 125 Ω/sq for monolayer graphene [3]. Additionally, as mentioned above, commonly applied PMMA based method is not suitable for large-scale industrial fabrication. Although commercially available ITO exhibits a very low sheet resistance (~10 Ω/sq), its transmission is as low as 84% [39]. Graphene films fabricated with the direct transfer employing parylene in this work have transmittance of ~96.5% and sheet resistance of 18 Ω/sq, which is the state-of-the-art combination of high transmittance and low sheet resistance.

Moreover, bare parylene showed 95% of transmittance which can be compared with the highest glass ~94% and PET ~90% transmittance at 550 nm wavelength [42]. Due to conformality of the CVD deposition process, parylene follows the surface morphology of the graphene on Cu film. Thus, final graphene/parylene film replicates initial roughness of the as-grown graphene/Cu foil. Electrochemical polishing of the Cu foil before the CVD growth of graphene to decrease roughness resulted in a dramatic enhancement in the transmittance of the graphene/parylene film up to 91%, which is correlated to a highest obtained graphene film transmittance of 96.5% (figure 4(b)).

2.4. Strain analysis of graphene films

As flexibility is an intrinsic property of graphene compared to fragile ITO, the electromechanical properties of graphene on parylene were also characterized. We verified the flexibility of graphene/parylene film by decreasing the bending radius from several centimeters to sub-millimeters. Figure 4(d) shows that the sheet resistance of the graphene/parylene film is practically unaffected by bending even to a radius of 0.25 mm. Strain S was calculated by

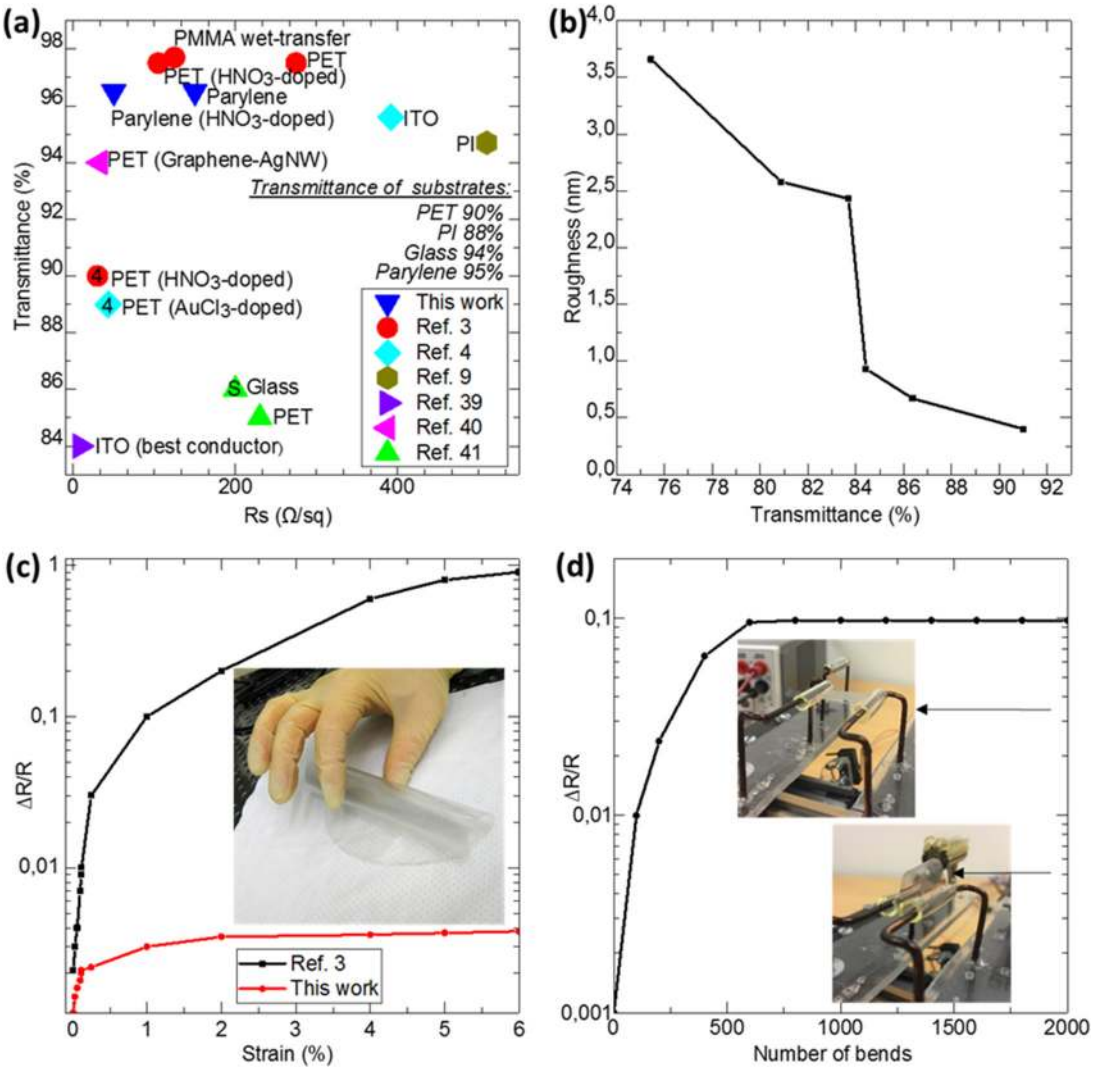

Figure 4. Transmission and strain analysis: (a) comparison to previous results of R_s versus T% plot for graphene only. Transmittance values are substrate normalized, i.e. refer to the characteristic of the conductive layer only. (b) Dependence of graphene/parylene film transmittance on Cu foil roughness. (c) Log-scaled $\Delta R/R$ versus strain. The inset shows rolled parylene/graphene film. (d) Log-scaled $\Delta R/R$ versus bending number (the repeated strain ~2%) for graphene/parylene film. The inset are photographs of the bending test.

$$S = \frac{t_s + t_f}{2R_b} \quad (2)$$

Where t_s, t_f, and R_b are the thickness of the substrate (parylene), the thickness of the conductive film (graphene), and the bending radius, respectively. As the monolayer graphene is extremely thin ($t_s \gg t_f$) we get

$$S = \frac{t_s}{2R_b} \quad (3)$$

When the film was fully folded, what corresponded to maximum applied strain (figure 4(c)), the sheet resistance was increased by less than 1% and, moreover, showed complete recovery after the strain was relaxed. The CVD graphene transferred on PET using the roll-to-roll method showed a 100% increase in a resistance under 6% strain [3]. Studies on conductive electrodes such as ITO and metal nanowire networks report resistance increase of more than 30% and permanent cracking under 4% strain [43–45]. Extreme flexibility is one of the advantages of the graphene/parylene film compared to alternative approaches. Moreover, graphene/parylene films showed high tolerance to tapping test (see supporting information figure S2). Authors wishing to acknowledge assistance or encouragement from colleagues, special work by technical staff or financial support from organizations should do so in an unnumbered Acknowledgments section immediately following the last numbered section of the paper.

3. Flexible electronics

Solvent-free transfer method demonstrated in this paper and bio-approved substrate allow using graphene/parylene films in wide array of wearable sensors and biological detectors. Moreover, in recent years a lot of efforts has been devoted to a novel type of energy harvesting technology called triboelectric nanogenerator (TENG), which can also be used as a

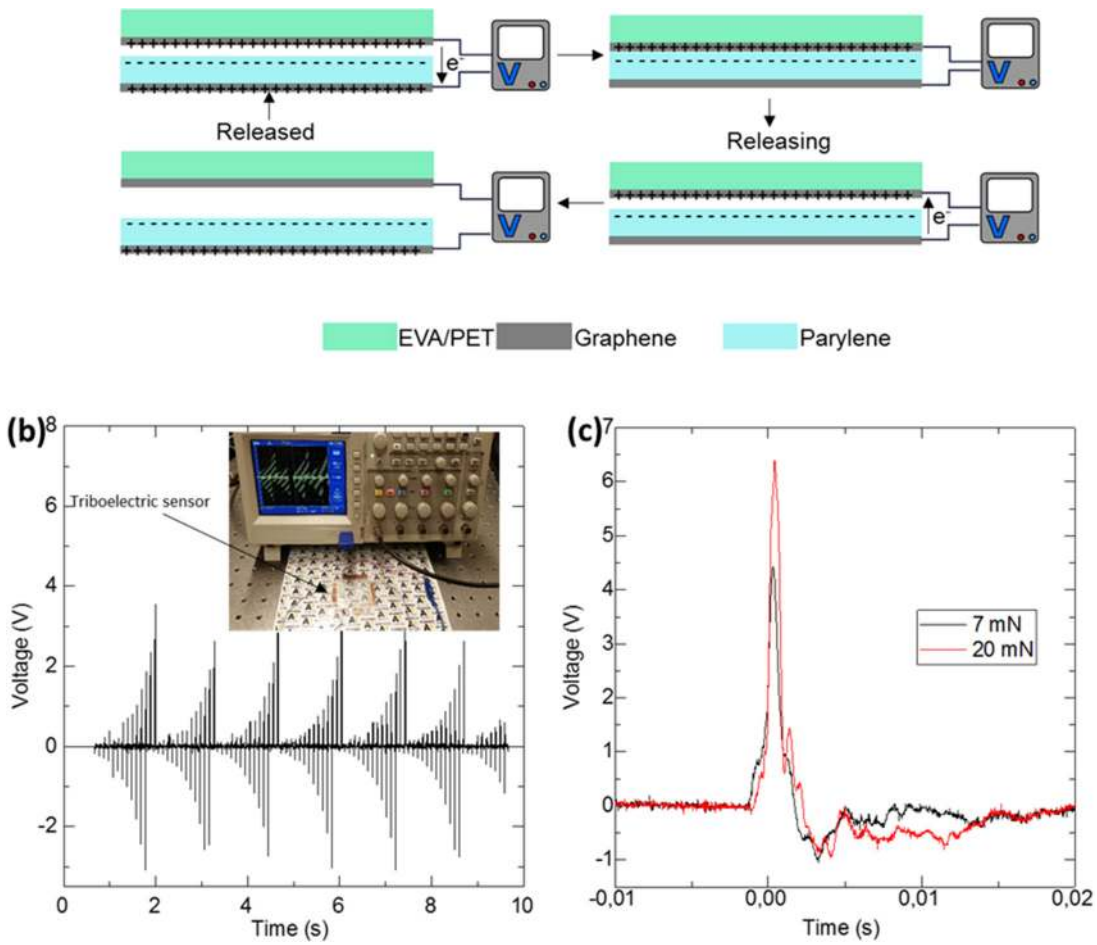

Figure 5. Triboelectric sensor based on graphene/parylene film: (a) schematic diagram of graphene/parylene based triboelectric sensor and working mechanism of the triboelectric sensor. (b) Output voltage measured under vertical compressive force. The inset photograph shows working triboelectric sensor with the size of 3 × 3 cm. (c) Output voltage measured under different forces.

self-powered sensor. Materials used for TENGs play an important role, as nanogenerators should serve as light weight, small size, low cost, flexible devices. Figure 5(a) shows a schematic diagram of a triboelectric sensor as one of possible graphene application (see supplementary video S3). The triboelectric effect appears while bringing into a physical contact two films with distinct electron affinity [46]. The upper layer consists of parylene/graphene film, and the bottom layer is graphene/EVA/PET film. Graphene here plays a role of the electrode and additionally as a friction layer, thus a high strain tolerance and high conductivity determine the device performance [14]. We utilized a thin PET net as a spacer for simplicity. However, high flexibility of the films enables to fabricate arch-shape sensors using such design as a spacer. Moreover, device reliability under strain was confirmed by testing more than 2000 cycles (figure 4(d)).

Various structures of TENGs with different working modes among with theoretical models have been published in recent years [46, 47]. The basic working principles of the triboelectric sensor is illustrated in figure 5(a). Full separation of the upper and bottom layer relates to initial neutral charge state. When the layers are brought into a contact using a vibrator, according to the triboelectric tendency, the negative electrostatic charges are generated at parylene/graphene film and positive at graphene/EVA/PET. Electron flow between the upper and bottom electrodes stops, when the opposite film polarities and produced charges are equalized. Releasing from fully pressed state starts to form a dipole moment due to the separation of opposite triboelectric charges, driving electron to flow from bottom to upper electrode. The flow stops at the maximum separation. Next pressing and releasing series will induce reverse flow of electrons between the electrodes when the dipole moment disappears. The contact electrification and following electrostatic induction process produces the output signals. Figure 5(b) shows output voltage under vertical compressive force with the vibrational frequency of ~8 Hz; the inset photograph shows triboelectric sensor with the size of 3 × 3 cm. Graphene-based triboelectric sensor showed high dependence of sensitivity under applied forces (figure 5(c)). It is important to notice that the 7 mN and 20 mN forces correspond to the force of 70 mg object falling from rest 10 cm and 30 cm, respectively. We also utilize our graphene films as transparent controllers (see Supplementary Video S4) and heaters (see supporting information figure S3 and supplementary video S5).

In conclusion, we have developed and demonstrated a wafer-scale direct transfer of monolayer CVD graphene onto a highly flexible and transparent substrate. Wet chemical doping significantly decreases sheet resistance and improves the spatial homogeneity of obtained films. Combined transmission and sheet resistance values of our graphene/parylene films are superior than the commonly used transparent electrodes such as ITO. Films have demonstrated the excellent stability of electromechanical properties against large bending deformations. Finally, we utilized graphene/parylene film for several original applications, such as a triboelectric sensor, transparent controllers, and flexible heaters. Moreover, this direct transfer concept can be readily adopted in production as parylene, which is well suited for batch processing and is already widely used for example in semiconductor and biomedical industry.

4. Methods

4.1. CVD growth of graphene

Growth of large-area monolayer graphene was carried out by commercial CVD system (Black Magic CVD system Aixtron BM6) and home-built rapid photothermal CVD system [48]. Commercial Cu foils (25 μm, 99.8% purity, Alfa Aesar product 7440508) were used as the substrate. Typical growth process in Black Magic CVD system was performed at a constant pressure of 4.1 mbar. First, Cu foil was annealed for 30 min at 850 °C using a 20 sccm flow of H_2 diluted by 1500 sccm of Ar. Reduction step was followed by a 10 min graphene deposition at 1025 °C by introducing additional 7 sccm of CH_4. Subsequently, the CH_4 flow was closed, and the chamber was cooled to a temperature below 150 °C and opened to ambient air. Electropolishing in orthophosphoric acid for 15 min removed tarnishing and roughness of Cu surface. The electrolytic solution was prepared using 55% H_3PO_4 and two-Cu-electrode system was polarized by −1.5 V.

4.2. Graphene/parylene films preparation

Parylene-C deposition was carried out in a commercially available deposition system PDS-2010 Labcoater 2 (Specialty Coating Systems). 25 g and 15 g of di-para-xylylene (Parylene-C dimer) were used to conformally deposit 25 μm and 15 μm films, respectively. An aqueous solution of NaOH was employed for electrochemical delamination (bubbling transfer) as an electrolyte while Cu was polarized at −5 V to delaminate parylene/graphene.

4.3. Characterizations

Confocal μ-Raman spectroscopy measurements were performed using commercial confocal Raman system Witec alpha300 RA with a green laser (532 nm). Hall system used to perform measurements by van der Pauw method had a sample size of 2 × 2 cm^2 and it operated at a room temperature in ambient air, with the magnetic field strength of 1 T.

Acknowledgments

The research leading to these results received funding from the European Union Horizon 2020 Programme under grant agreement 696656 Graphene Core. This was undertaken at the Micronova, Nanofabrication Center of Aalto University.

References

[1] Novoselov K S, Geim A K, Morozov S V, Jiang D, Zhang Y, Dubonos S V, Grigorieva I V and Firsov A A 2004 Electric field effect in atomically thin carbon films *Science* **306** 666–9
[2] Singh V, Joung D, Zhai L, Das S, Khondaker S I and Seal S 2011 Graphene based materials: past, present and future *Prog. Mater. Sci.* **56** 1178–271
[3] Bae S *et al* 2010 Roll-to-roll production of 30-inch graphene films for transparent electrodes *Nat. Nanotechnol.* **5** 574–8
[4] Kang J, Kim H, Kim K S, Lee S, Bae S, Ahn J, Kim Y, Choi J and Hong B H 2011 High-performance graphene-based transparent flexible heaters *Nano Lett.* **11** 5154–8
[5] Schwierz F 2010 Graphene transistors *Nat. Nanotechnol.* **5** 487–96
[6] Nair R R, Blake P, Grigorenko A N, Novoselov K S, Booth T J, Stauber T, Peres N M R and Geim A K 2008 Fine structure constant defines visual transparency of graphene *Science* **320** 1308
[7] Li X, Cai W, An J, Kim S, Nah J, Yang D, Colombo L and Ruoff R S 2009 Large area synthesis of high-quality and uniform graphene films on copper foils *Science* **324** 1312–4
[8] Martins L G P, Song Y, Zeng T, Dresselhaus M S, Kong J and Araujo P T 2013 Direct transfer of graphene onto flexible substrates *Proc. Natl Acad. Sci. USA* **110** 17762–7
[9] Chen T L, Ghosh D S, Marchena M, Osmond J and Pruneri V 2015 Nanopatterned graphene on a polymer substrate by a direct peel-off technique *ACS Appl. Mater. Interfaces* **7** 5938–43
[10] Cherian C T, Giustiniano F, Martin-Fernandez I, Andersen H, Balakrishnan J and Özyilmaz B 2015 'Bubble-free' electrochemical delamination of CVD graphene films *Small* **11** 189–94
[11] Zhang Z, Du J, Zhang D, Sun H, Yin L, Ma L, Chen J, Ma D, Cheng H and Ren W 2017 Rosin-enabled ultraclean and damage-free transfer of graphene for large-area flexible organic light-emitting diodes *Nat. Commun.* **8** 14560
[12] Kang J, Hwang S, Kim J H, Kim M H, Ryu J and Seo S J 2012 Efficient transfer of large-area graphene films onto rigid substrates by hot pressing *ACS Nano* **6** 5360–5
[13] Chen Y, Gong X and Gai J 2016 Progress and challenges in transfer of large-area graphene films *Adv. Sci.* **3** 1500343
[14] Chandrashekar B N, Deng B, Smitha A S, Chen Y, Tan C, Zhang H, Peng H and Liu Z 2015 Roll-to-roll green transfer of CVD graphene onto plastic for a transparent and flexible triboelectric nanogenerator *Adv. Mater.* **27** 5210–6
[15] Na S R, Suk J W, Tao L, Akinwande D, Ruoff R S and Huang R 2015 Selective mechanical transfer of graphene from seed copper foil using rate effects *ACS Nano* **9** 1325–35
[16] Senkevich J J, Wiegand C J, Yang G and Lu T 2004 Selective deposition of ultrathin poly(p-xylylene) films on dielectrics versus copper surfaces *Chem. Vapor Depos.* **10** 247–9
[17] Chang T Y, Yadav V G, De Leo S, Mohedas A, Rajalingam B, Chen C L, Selvarasah S, Dokmeci M R and Khademhosseini A 2007 Cell and protein compatibility of parylene-C surfaces *Langmuir* **23** 11718–25
[18] Trantidou T, Tariq M, Terracciano C M, Toumazou C and Prodromakis T 2014 Parylene C-based flexible electronics for pH monitoring applications *Sensors* **14** 11629–39

[19] Park D et al 2016 Fabrication and utility of a transparent graphene neural electrode array for electrophysiology, in vivo imaging, and optogenetics Nat. Protocols 11 2201–22
[20] Bareket-Keren L and Hanein Y 2013 Carbon nanotube-based multi electrode arrays for neuronal interfacing: progress and prospects Front. Neural Circuits 6 122
[21] Chen C L, Lopez E, Jung Y J, Muftu S, Selvarasah S and Dokmeci M R 2008 Mechanical and electrical evaluation of parylene-C encapsulated carbon nanotube networks on a flexible substrate Appl. Phys. Lett. 93 093109
[22] Skoblin G, Sun J and Yurgens A 2017 Encapsulation of graphene in parylene Appl. Phys. Lett. 110 3–7
[23] Sabri S S, Levesque P L, Aguirre C M, Guillemette J, Martel R and Szkopek T 2009 Graphene field effect transistors with parylene gate dielectric Appl. Phys. Lett. 95 10–3
[24] Chamlagain B et al 2014 Mobility improvement and temperature dependence in $MoSe_2$ field-effect transistors on parylene-C substrate ACS Nano 8 5079–88
[25] Park D W, Kim H, Bong J, Mikael S, Kim T J, Williams J C and Ma Z 2016 Flexible bottom-gate graphene transistors on Parylene C substrate and the effect of current annealing Appl. Phys. Lett. 109 152105
[26] Yoon Y S et al 2006 Effects of parylene buffer layer on flexible substrate in organic light emitting diode Thin Solid Films 513 258–63
[27] Tan C P and Craighead H G 2010 Surface engineering and patterning using parylene for biological applications Materials 3 1803–32
[28] Ferrari A C and Basko D M 2013 Raman spectroscopy as a versatile tool for studying the properties of graphene Nat. Nanotechnol. 8 235–46
[29] Bouleghlimat E, Davies P R, Davies R J, Howarth R, Kulhavy J and Morgan D J 2013 The effect of acid treatment on the surface chemistry and topography of graphite Carbon 61 124–33
[30] Howard C, Dean M P M and Withers F 2011 Phonons in potassium-doped graphene: the effects of electron–phonon interactions, dimensionality, and adatom ordering Phys. Rev. B 84 241404
[31] Kalita G, Wakita K, Takahashi M and Umeno M 2011 Iodine doping in solid precursor-based CVD growth graphene film J. Mater. Chem. 21 15209–13
[32] Kim K K, Reina A, Shi Y, Park H, Li L, Lee Y H and Kong J 2010 Enhancing the conductivity of transparent graphene films via doping Nanotechnology 21 285205
[33] Kim H, Renault O, Tyurnina A, Simonato J, Rouchon D, Mariolle D, Chevalier N and Dijon J 2014 Doping efficiency of single and randomly stacked bilayer graphene by iodine adsorption Appl. Phys. Lett. 105 011605
[34] Li S, Lijie C, Wei G and Pulickel M A 2009 Transfer printing of graphene using gold film ACS Nano 3 1353–6
[35] Kwon K C, Choi K S, Kim C and Kim S Y 2014 Role of metal cations in alkali metal chloride doped graphene J. Phys. Chem. C 118 8187–93
[36] Das S, Sudhagar P, Ito E, Lee D, Nagarajan S, Lee S Y, Kang Y S and Choi W 2012 Effect of HNO_3 functionalization on large scale graphene for enhanced tri-iodine reduction in dye-sensitized solar cells J. Mater. Chem. 22 20490–7
[37] De S and Coleman J N 2010 Are there fundamental limitations on the sheet resistance and transmittance of thin graphene films ACS Nano 4 2713–20
[38] Bao W et al 2014 Approaching the limits of transparency and conductivity in graphitic materials through lithium intercalation Nat. Commun. 5 4224
[39] Yu K and Chen J 2014 Graphene-based transparent conductive electrodes Mater. Matters 9 6–13
[40] Lee M et al 2013 High-performance, transparent, and stretchable electrodes using graphene-metal nanowire hybrid structures Nano Lett. 13 2814–21
[41] Zhang Y I, Zhang L and Zhou C 2013 Review of chemical vapor deposition of graphene and related applications Acc. Chem. Res. 46 2329–39
[42] Jeong Y S, Ratier B, Moliton A and Guyard L 2002 UV-visible and infrared characterization of poly(p-xylylene) films for waveguide applications and OLED encapsulation Synth. Met. 127 189–93
[43] He T, Xie A, Reneker D H and Zhu Y 2014 A tough and high-performance transparent electrode from a scalable and transfer-free method ACS Nano 8 4782–9
[44] Peng C, Jia Z, Neilson H, Li T and Lou J 2012 In situ electro-mechanical experiments and mechanics modeling of fracture in indium tin oxide-based multilayer electrodes Adv. Eng. Mater. 15 250–6
[45] Bao C et al 2015 In situ fabrication of highly conductive metal nanowire networks with high transmittance from deep-ultraviolet to near-infrared ACS Nano 9 2502–9
[46] Wang Z L, Chen J and Lin L 2015 Progress in triboelectric nanogenerators as a new energy technology and self-powered sensors Energy Environ. Sci. 8 2250–82
[47] Wang Z L 2014 Triboelectric nanogenerators as new energy technology and self-powered sensors—principles, problems and perspectives Faraday Discuss. 176 447–58
[48] Riikonen J, Kim W, Li C, Svensk O, Arpiainen S, Kainlauri M and Lipsanen H 2013 Photo-thermal chemical vapor deposition of graphene on copper Carbon 62 43–50